JCB Article

Functional characterization of the KNOLLE-interacting t-SNARE AtSNAP33 and its role in plant cytokinesis

Maren Heese,[1] Xavier Gansel,[2] Liliane Sticher,[2] Peter Wick,[2] Markus Grebe,[1] Fabienne Granier,[3] and Gerd Jürgens[1]

[1]Zentrum für Molekularbiologie der Pflanzen, Universität Tübingen, D-72076 Tübingen, Germany
[2]Université de Fribourg, Département de Biologie, Unité de Biologie Végétale, CH-1700 Fribourg, Switzerland
[3]Station de Génétique et Amélioration des Plantes, Institut National de la Recherche Agronomique-Centre de Versailles, F-78026 Versailles Cedex, France

Cytokinesis requires membrane fusion during cleavage-furrow ingression in animals and cell plate formation in plants. In *Arabidopsis*, the Sec1 homologue KEULE (KEU) and the cytokinesis-specific syntaxin KNOLLE (KN) cooperate to promote vesicle fusion in the cell division plane. Here, we characterize AtSNAP33, an *Arabidopsis* homologue of the t-SNARE SNAP25, that was identified as a KN interactor in a yeast two-hybrid screen. AtSNAP33 is a ubiquitously expressed membrane-associated protein that accumulated at the plasma membrane and during cell division colocalized with KN at the forming cell plate. A T-DNA insertion in the *AtSNAP33* gene caused loss of AtSNAP33 function, resulting in a lethal dwarf phenotype. *atsnap33* plantlets gradually developed large necrotic lesions on cotyledons and rosette leaves, resembling pathogen-induced cellular responses, and eventually died before flowering. In addition, mutant seedlings displayed cytokinetic defects, and *atsnap33* in combination with the cytokinesis mutant *keu* was embryo lethal. Analysis of the *Arabidopsis* genome revealed two further SNAP25-like proteins that also interacted with KN in the yeast two-hybrid assay. Our results suggest that AtSNAP33, the first SNAP25 homologue characterized in plants, is involved in diverse membrane fusion processes, including cell plate formation, and that AtSNAP33 function in cytokinesis may be replaced partially by other SNAP25 homologues.

Introduction

Cytokinesis completes the process of cell division by forming new membranes that partition the cytoplasm among the daughter cells. Although other aspects of cell division are highly conserved, cytokinesis appears to be carried out very differently between animals and plants (Glotzer, 1997). In animals, a contractile actomyosin-based ring marks the margin of the ingrowing plasma membrane, which closes like a diaphragm in between the newly formed nuclei (Straight and Field, 2000). The ingression of the cleavage furrow is supported by vesicle fusion that inserts new membrane material behind the leading edge (Lecuit and Wieschaus, 2000). By contrast, somatic cytokinesis of higher plants starts in the center of a dividing cell with the de novo formation of a disk-shaped membrane compartment, the cell plate, that grows centrifugally, eventually fusing with the parental plasma membrane (Otegui and Staehelin, 2000). Formation and lateral expansion of the cell plate are brought about by the fusion of Golgi-derived vesicles, initially with one another and later with the margin of the growing cell plate. Thus, although cytokinesis appears to be different between animal and plant cells membrane fusion is required in both (O'Halloran, 2000). However, not much is known in either system about the molecules driving this process.

The machinery of membrane fusion shows a high degree of conservation across eukaryotes and has been studied in a variety of systems (for reviews see Blatt et al., 1999; Pelham, 1999; Lin and Scheller, 2000). Recent models propose that the initial contact between two membrane compartments is made by tethering protein complexes that differ in composition, depending on the membranes involved (Waters and Hughson, 2000). Subsequently, membrane docking occurs, mediated by the formation of a four-helical bundle of membrane-associated soluble *N*-ethylmaleimide–sensitive factor attachment

Address correspondence to Gerd Jürgens, Zentrum für Molekularbiologie der Pflanzen, Universität Tübingen, Auf der Morgenstelle 3, D-72076 Tübingen, Germany. Tel.: 49-7071-2978887. Fax: 49-7071-295797. E-mail: gerd.juergens@zmbp.uni-tuebingen.de

M. Grebe's present address is Dept. of Molecular Cell Biology, Utrecht University, NL-3584 CH Utrecht, Netherlands.

Key words: *Arabidopsis*; cytokinesis; vesicle trafficking; SNARE complex; SNAP25

protein receptor (SNARE)* proteins. One helix of this trans-SNARE complex is contributed by a vesicle SNARE (v-SNARE) anchored to one membrane compartment, and three helices are added by target membrane SNAREs (t-SNAREs) residing on the other compartment. The t-SNAREs always include a syntaxin, which contributes one helix, whereas the remaining two helices are either from a single SNAP25-type protein or from two separate t-SNARE light chains. Trimeric SNARE complexes involving a SNAP25 homologue have been described in plasma membrane fusion events, whereas tetrameric SNARE complexes prevail in endomembrane fusion processes (Fukuda et al., 2000). To what degree the large class of SNARE proteins contributes to the specificity of membrane fusion processes is still an open question. It has been proposed that possible fusion events are limited by SNARE compatibility and are further restricted in vivo by additional proteins (McNew et al., 2000).

Although SNAREs are sufficient for membrane docking and fusion in vitro (Weber et al., 1998), several regulatory proteins are necessary for trans-SNARE complex formation in vivo. One class of regulators are the Sec1-type proteins. As revealed by x-ray crystallography, neuronal Sec1 binds Syntaxin 1A in a "closed" conformation unsuitable for interaction with other SNAREs and thus may prevent inappropriate SNARE complex formation (Misura et al., 2000). However, yeast Sec1p has been shown to associate with the assembled SNARE core complex (Carr et al., 1999), which suggests several functions for Sec1 or different roles in different systems.

Animal and plant mutants defective in the execution of cytokinesis have been related to genes encoding components of the vesicle fusion machinery. Cellularization of the *Drosophila* embryo is impaired in *syntaxin1* mutants (Burgess et al., 1997), and the cleavage furrow fails to ingress properly in *syntaxin-4* knockout embryos of *Caenorhabditis elegans* (Jantsch-Plunger and Glotzer, 1999). Both syntaxins have been localized to the ingrowing plasma membrane, implying a direct role in membrane addition during cytokinesis. In *Arabidopsis*, mutations in the *KNOLLE (KN)* or *KEULE (KEU)* genes cause strong cytokinetic defects, such as enlarged partially divided multinucleate cells, that are already apparent during embryogenesis and result in seedling lethality (Assaad et al., 1996; Lukowitz et al., 1996). In both mutants, unfused vesicles accumulate in the plane of cell division (Lauber et al., 1997; Waizenegger et al., 2000), suggesting a defect in cytokinetic vesicle fusion. KN belongs to the syntaxin family of proteins and has been shown to localize to the forming cell plate (Lauber et al., 1997). Whereas *KN* expression is confined to dividing cells, *KEU*, which codes for a Sec1 homologue, is expressed more broadly and appears to be involved also in processes other than cytokinesis such as root hair elongation (Assaad et al., 2001). Although several other plant genes with cytokinesis-defective mutant phenotypes have been cloned (for review see Nacry et al., 2000), none encodes an additional component of the membrane fusion machinery. Thus, there are still fundamental questions to be answered. Is the presumed cytokinetic SNARE complex trimeric, tetrameric, or completely different in composition? Are SNAREs other than KN also cytokinesis specific? To identify more components involved in cytokinetic vesicle fusion, we searched for KN-interacting proteins using the yeast two-hybrid system. Here, we report the functional characterization of the KN interactor AtSNAP33 (SNP33), an *Arabidopsis* SNAP25-type t-SNARE of 33 kD.

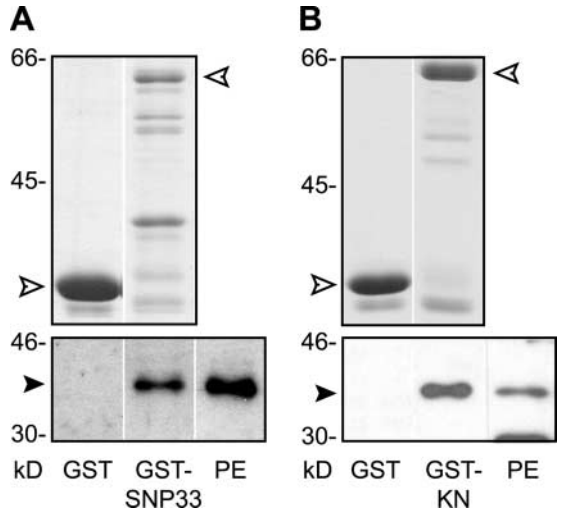

Figure 1. **Binding of SNP33 and KN in vitro.** GST fusion proteins were used to precipitate interacting partners from suspension culture extracts of *Arabidopsis*. GST alone served as a negative control. One third of each precipitate was analyzed by Coomassie-stained gels (top). Note that the amount of GST was the same or more than the amount of GST fusion protein in both assays (white arrowheads). Western blots were used to test for coprecipitated proteins (bottom). PE is an aliquot of the suspension culture extract used for the assay. Black arrowheads indicate sizes of KN (A) and SNP33 (B). (A) Pull-down with GST-SNP33 detected by anti-KN serum; 1/10 of the precipitates and 1/200 of the plant extract (PE) were loaded. (B) Pull-down with GST-KN detected by anti-SNP33 serum; 1/8 of the precipitates and 1/300 of the plant extract were loaded.

Results

AtSNAP33 interacts with the cytokinesis-specific syntaxin KN

SNARE-mediated membrane fusion plays an important role in plant cytokinesis as indicated by the characterization of the Sec1 homologue KEU and the cytokinesis-specific syntaxin KN from *Arabidopsis*. To identify additional members of the presumed SNARE complex involved in cytokinetic vesicle fusion, we performed a yeast two-hybrid screen using the cytoplasmic domain of KN as the "bait" and a "prey" cDNA library prepared from young siliques. Among 1.8 million primary transformants, three independent partial clones derived from the same gene, the *SNAP25* homologue *AtSNAP33* (*SNP33*), were identified as strong KN interactors.

*Abbreviations used in this paper: BFA, brefeldin A; GFP, green fluorescent protein; GST, glutathione *S*-transferase; KEU, KEULE; KN, KNOLLE; SNARE, soluble *N*-ethylmaleimide–sensitive factor attachment protein receptor; SNP33, AtSNAP33; t-SNARE, target membrane SNARE; v-SNARE, vesicle SNARE.

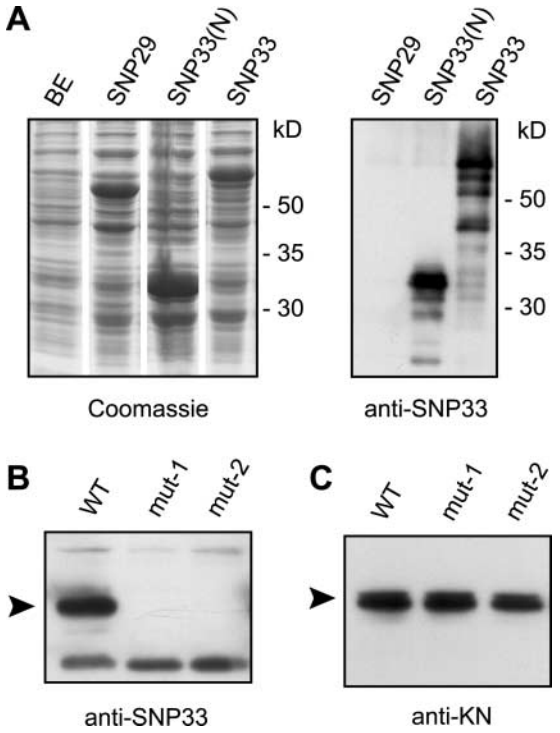

Figure 2. **Characterization of an antiserum raised against SNP33.** (A) The anti-SNP33 serum was tested on extracts from bacteria expressing GST-SNP33 (SNP33), an NH_2-terminal fragment of SNP33 fused to GST (SNP33(N)) or a GST fusion of the related AtSNAP29 (SNP29). The left panel shows a Coomassie-stained gel to compare the amounts of total protein loaded. BE, bacterial extract without recombinant protein. For the Western blot (right panel), 1:200 dilutions of the extracts were used. (B and C) Total protein extracts from wild-type (WT) and two *snp33* (mut-1 and mut-2) mutant callus cultures were separated on SDS-PAGE gels, transferred to PVDF membranes, and detected with anti-SNP33 serum (B) or anti-KN serum (C, control). The arrowheads mark the sizes of the expected proteins. KN expression was the same in all extracts, indicating equal loading. A band of about 33 kD was detected by the anti-SNP33 serum in wild-type but not in *snp33* mutant extracts.

The *SNP33* full-length cDNA encodes a 300 amino acid hydrophilic protein with a deduced molecular weight of 33.6 kD. The COOH-terminal 200 amino acids of SNP33 show 28% identity and 50% similarity to human SNAP25 isoform B, and the regions of highest homology comprise the two α-helical domains required for SNARE core complex formation (see Fig. 9). To rule out artifactual interaction due to protein truncation, full-length *SNP33* cDNA was cloned into the prey vector and analyzed in the yeast two-hybrid assay. Consistently, SNP33 interacted only with KN but not with other unrelated baits (unpublished data).

Glutathione *S*-transferase GST pulldown experiments were performed to assess KN/SNP33 interaction in a different assay. An NH_2-terminal GST fusion of SNP33 bound to glutathione-coupled beads precipitated KN from an *Arabidopsis* suspension culture extract, whereas GST alone did not (Fig. 1 A). A polyclonal antiserum generated against full-length SNP33 (see below) enabled us to perform also the reciprocal experiment. SNP33 was detected in the pellet after precipitation with GST-KN but not with GST alone (Fig. 1 B). In addition, GST-SNP33 specifically precipitated bacterially ex-

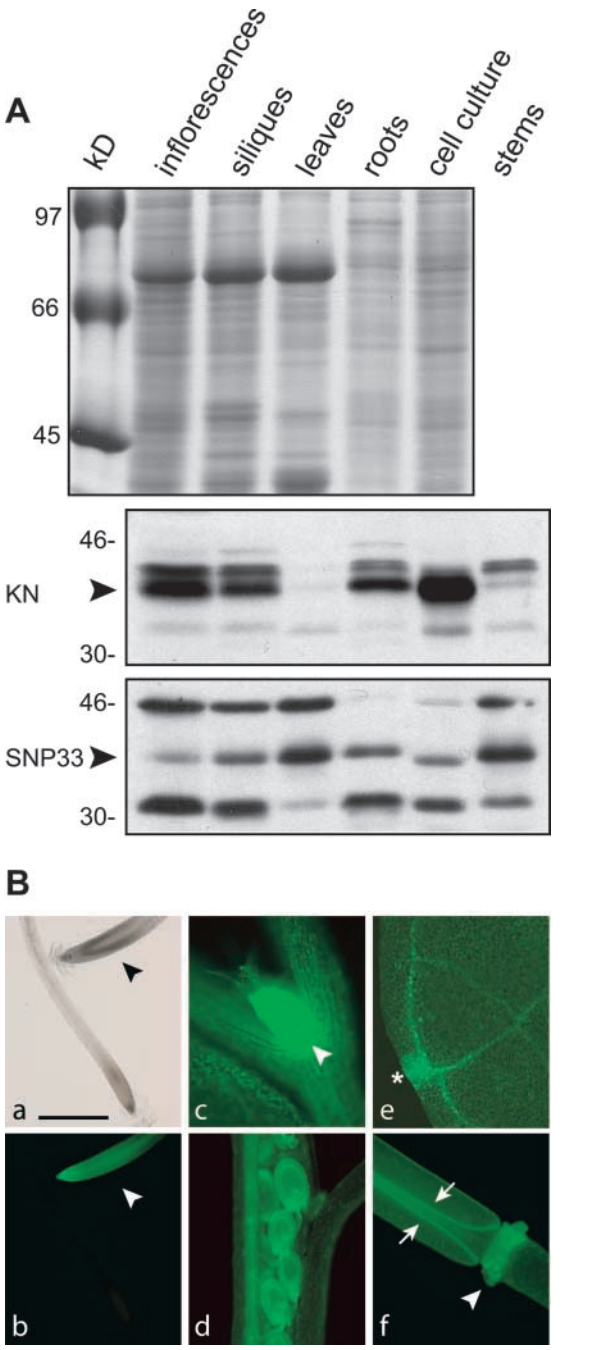

Figure 3. **Ubiquitous expression of SNP33.** (A) Total protein extracts of different organs were separated by SDS-PAGE, transferred to PVDF membranes, and detected with anti-KN serum (second panel; arrowhead, size of KN) or anti-SNP33 serum (third panel; arrowhead, size of SNP33). A Coomassie-stained gel (top) is shown as loading control; protein concentration of stem extract was adjusted to that of cell culture extract based on another Coomassie-stained gel (unpublished data). (B) Expression of GFP under the control of a 2.1-kb genomic fragment containing the *SNP33* promotor (Fig. 4, fragment C) was analyzed. Examples of tissues with strong GFP fluorescence are shown. (a and b) Transgenic root (arrowhead) next to a wild-type root shown in bright field (a) and fluorescence using a GFP filter (b). (c) Young leaves emerging between the petioles of the cotyledons (arrowhead). (d) Ovules in an opened silique. (e) Vascular tissue and hydathode (asterisk) of a cotyledon. (f) Abscission (arrowhead) and dehiscence zones (arrows) of a silique. Bar: (a–d) 150 μm; (e) 75 μm; (f) 950 μm.

pressed $(His)_6$-KN, implying that no other plant proteins are needed for KN/SNP33 interaction (unpublished data).

SNP33 is ubiquitously expressed

For interaction to occur in vivo, SNP33 and KN need to be expressed in overlapping domains. To test for SNP33 expression, we generated a polyclonal antiserum against the full-length protein. The antiserum recognized different forms of recombinant SNP33 protein but not the related AtSNAP29 (Fig. 2 A). On Western blots of plant extracts, a band corresponding to the predicted size of SNP33 was detected. This band was only present in wild-type extracts but not in extracts from a *snp33* T-DNA insertion mutant (see below), confirming the specificity of the anti-SNP33 antiserum (Fig. 2 B).

To compare SNP33 and KN expression, protein blots of extracts from different organs were probed with both antisera (Fig. 3 A). KN expression was restricted to organs containing proliferating tissues as reported previously (Lauber et al., 1997). By contrast, SNP33 seemed to be expressed in all organs analyzed. The expression level in leaves was variable, ranging from barely detectable to high. The reason for this variability of expression, which was observed repeatedly, is not known.

To better resolve the pattern of *SNP33* gene expression, *green fluorescent protein (GFP)* was fused transcriptionally to a 2.1-kb fragment of the *SNP33* promoter region (Fig. 4, construct C). Several independent transgenic *Arabidopsis* lines were tested for GFP expression by fluorescence microscopy, which revealed low level expression in all tissues analyzed (unpublished data). Especially strong fluorescence was observed in root tips, ovules, very young leaves, vascular tissue, hydathodes, stipules, and the abscission and dehiscence zones of the siliques. Examples of tissues with strong expression are shown in Fig. 3 B. In summary, ubiquitous expression of SNP33 allows for in vivo interaction with KN but also suggests other functions unrelated to cytokinesis.

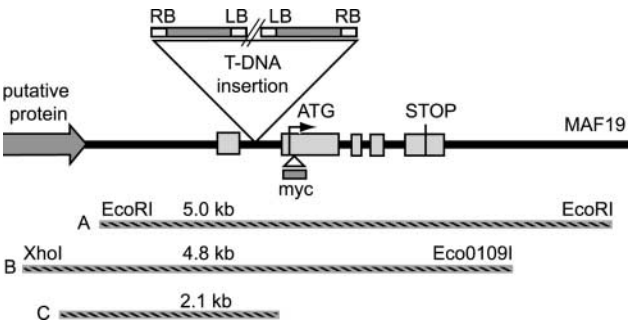

Figure 4. **Schematic representation of the *SNP33* genomic region.** (Top) The black bar represents the genomic region of *SNP33* on chromosome 5 (P1 clone MAF19). The five exons of *SNP33* are depicted as light grey boxes, and the initiating ATG and the stop codon are indicated. The arrow on the left represents a neighboring gene. Triangles indicate the sites of T-DNA and myc-tag insertions (not drawn to scale). (Bottom) The hatched bars represent genomic fragments used for different constructs (lengths and terminal restriction sites are indicated). A and B were used to rescue the *snp33* mutant, and C was transcriptionally fused to GFP for expression analysis of *SNP33*. Note that fragment C comprises a larger 5′ region than rescue construct A and thus likely contains the complete *SNP33* promoter.

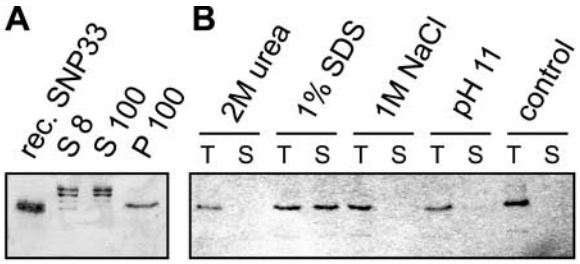

Figure 5. **SNP33 is associated with membranes.** (A) Cell fractionation of in vitro–cultured *Arabidopsis* roots. S8, supernatant of 8,000 *g* precentrifugation; S 100 and P 100, supernatant and pellet of 100,000 *g* ultracentrifugation; rec.SNP33, recombinant SNP33 protein used as a size standard. (B) Aliquots of the microsomal fraction (A, P 100) were extracted with the buffers indicated (0.1 M Na_2CO_3, pH 11; control, 10 mM phosphate buffer, pH 7.6). For each aliquot, total protein (T) before and supernatant (S) after a 100,000 *g* centrifugation were analyzed in Western blots to test for solubilization of SNP33.

Subcellular localization of SNP33 protein

To characterize more closely the in vivo function of SNP33, we analyzed its subcellular localization by cell fractionation and immunofluorescence microscopy. As shown in Fig. 5 A, SNP33 was detected in the pellet after a 100,000 *g* centrifugation step, indicating its association with membranes. Comparable results had been reported for other SNAP25 homologues, although proteins of this family lack a membrane-spanning domain (Brennwald et al., 1994; Steegmaier et al., 1998). To examine how tightly SNP33 was associated with membranes, the pellet of the 100,000 *g* centrifugation was resuspended in different buffers and recentrifuged (Fig. 5 B). SNP33 was released only by detergent but not by high salt, high pH, or urea and thus behaved like an integral membrane protein.

The anti-SNP33 serum was not suitable for immunolocalization of SNP33 protein. Therefore, we generated transgenic *Arabidopsis* plants expressing a myc-tagged version of SNP33. A nucleotide linker coding for the myc epitope was inserted into a unique SalI site of a 4.8-kb genomic *SNP33* fragment (Fig. 4, fragment B), which placed the epitope at amino acid 17 of the SNP33 protein. This construct rescued the *snp33* mutant (see below), suggesting that myc-SNP33 was fully functional.

All plants used for immunofluorescence experiments carried myc-SNP33 as the only functional version of the protein. Transgene expression was analyzed in whole-mount preparations of root tips using the monoclonal c-myc antibody 9E10 (Fig. 6). All cell layers of the root tip were labeled, confirming the ubiquitous SNP33 expression seen in *SNP33–GFP* reporter lines. Whereas no signal was detected in wild-type, *myc-SNP33* plants displayed clear labeling of the plasma membrane, which in most cases was accompanied by a weaker granular staining of the cytoplasm (Fig. 6, A–C).

Dividing cells were analyzed to investigate the role of AtSNAP33 in cytokinesis. Myc-SNP33 was found in a narrow band between the reforming daughter nuclei (Fig. 6 D). Furthermore, SNP33 colocalized with the KN syntaxin at the forming cell plate from early to late in division (Fig. 6, E–G). This observation strongly suggests an in vivo interac-

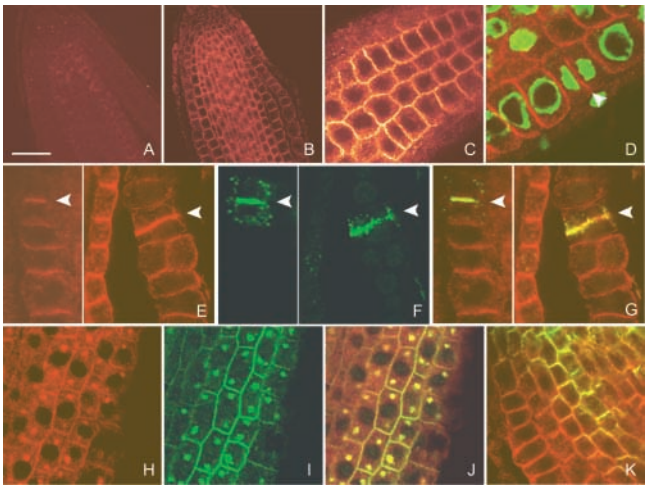

Figure 6. **Immunolocalization of SNP33 protein.** Root tips of wild-type control (A) and transgenic lines expressing myc-SNP33 (B–K) as the only functional version of the protein were analyzed by whole-mount immunofluorescence confocal microscopy. (A–D) Staining for myc-SNP33 (orange/red) and DNA (green, only in D). (A) No expression in wild-type. (B) Expression in all cells of the transgenic root tip. (C) Strong label at the plasma membrane. (D) Labeling of the cell plate (arrowhead) between daughter nuclei. (E–G) Dividing cells were double labeled for myc-SNP33 (E, red) and KN (F, green); overlays (G). Yellow signals in G indicate colocalization of myc-SNP33 and KN. The arrowheads mark early (left) and late (right) cell plates. (H–K) Double labeling for myc-SNP33 (H, red) and PIN1 (I, green); overlays (J and K). Yellow signals indicate colocalization. (H–J) Cells were treated with 100 μM BFA for 2 h. Note the accumulation of label in two distinct patches within the cells. (K) Untreated control cells. Bar: (A and B) 40 μm; (C and K) 15 μm; (D and H–J) 8 μm; (E–G) 10 μm.

tion of both proteins. Analysis of embryonic tissue revealed a subcellular distribution of SNP33 indistinguishable from that seen in the root tip (unpublished data), indicating that the localization of SNP33 is not tissue or developmental stage dependent.

Root tips were treated with brefeldin A (BFA) which blocks anterograde membrane trafficking and leads to an agglomeration of endomembranes (Satiat-Jeunemaitre and Hawes, 1992). Upon treatment, myc-SNP33 accumulated in large patches inside the cell, indicating that at least some of the cytoplasmic label is membrane bound. A similar distribution has been reported for the putative auxin-efflux carrier PIN1 in BFA-treated cells (Steinmann et al., 1999), and the resulting BFA compartment has been interpreted as a mixture of endosome and Golgi stacks (Satiat-Jeunemaitre and Hawes, 1992; Geldner et al., 2001). Colabeling revealed that both PIN1 and SNP33 accumulated in the same compartment (Fig. 6, H–K). In summary, SNP33 is a tightly membrane-associated protein that localizes to the plasma membrane and some endomembrane compartment and to the cell plate in dividing cells.

Identification of an *snp33* T-DNA insertion mutant

The SNP33/KN in vitro interaction and their in vivo colocalization strongly suggested a functional role for SNP33 at the cell plate. To test whether SNP33 function is indeed required for cytokinesis, we searched for mutants in the Versailles collection of *Arabidopsis* T-DNA insertion lines (Bechtold et al., 1993). We identified one line carrying an insertion in the first intron of *SNP33* that separates the transcriptional from the translational start site (Fig. 4). PCR and Southern blot analysis revealed that the insertion most likely consists of two T-DNAs in an inverted repeat conformation. The junctions of both T-DNA right borders with the intron sequences of *SNP33* were confirmed by sequencing (unpublished data).

A recessive mutant phenotype cosegregated with the T-DNA insertion (see below). To determine whether the mutant phenotype was caused by disruption of the *SNP33* gene, plants hemizygous for the T-DNA insertion were transformed with different constructs that contained the *SNP33* genomic region (Fig. 4) and a hygromycin-selectable marker. None of the >100 hygromycin-resistant T1 plants analyzed per construct displayed the mutant phenotype, although ~25% of these plants were homozygous for the T-DNA insertion in the endogenous *SNP33* gene. Furthermore, T1 plants that were heterozygous for the T-DNA insertion at the *SNP33* locus and carried one unlinked rescue construct segregated ~6.25% mutant seedlings, whereas T1 plants homozygous for the T-DNA insertion and carrying one unlinked rescue construct segregated ~25% mutant seedlings. Thus, the observed mutant phenotype was caused by T-DNA disruption of the *SNP33* gene. The overlap of the two smallest rescue constructs defines a 4.1-kb EcoRI/Eco0109I fragment to be sufficient for complementation, containing a 1.2 kb promoter and a 2.2 kb transcribed and a 0.7 kb 3′ region of the *SNP33* gene.

Phenotypic characterization of the *snp33* mutant

Macroscopically, *snp33* mutant seedlings could not be distinguished from wild-type until 7–9 d after germination (Fig. 7 A, left). At that time, brownish lesions appeared on the cotyledons, and the seedlings lagged behind in development. The lesions became more frequent and enlarged until the whole cotyledon turned necrotic. Subsequently, developing rosette leaves gradually formed lesions also, mostly starting at the leaf tip (Fig. 7 B). Although *snp33* mutants grown on agar plates continued to produce rosette leaves for several weeks, they hardly increased in size, resembling extreme dwarfs (Fig. 7 C). Eventually, cell death occurred also in the youngest leaves and in the hypocotyl, and the plantlets died before flowering.

The *snp33* phenotype was reminiscent of mutants collectively called disease lesion mimics that show spontaneous cell death in the absence of pathogens. A subclass of these mutants also mimic the cellular and molecular processes involved in plant disease response (Dietrich et al., 1994). Therefore, we tested *snp33* mutants for two easily accessible cellular markers, autofluorescence and callose deposition, which are often correlated with a plant–pathogen interaction. When analyzed in blue light, cells within the lesions showed bright yellow autofluorescence that slightly preceded browning (Fig. 7, G and H). Aniline blue staining to detect callose revealed subcellularly restricted cell wall appositions in mutant cotyledons that were enlarged significantly compared with those observed in wild-type (Fig. 7, I and J).

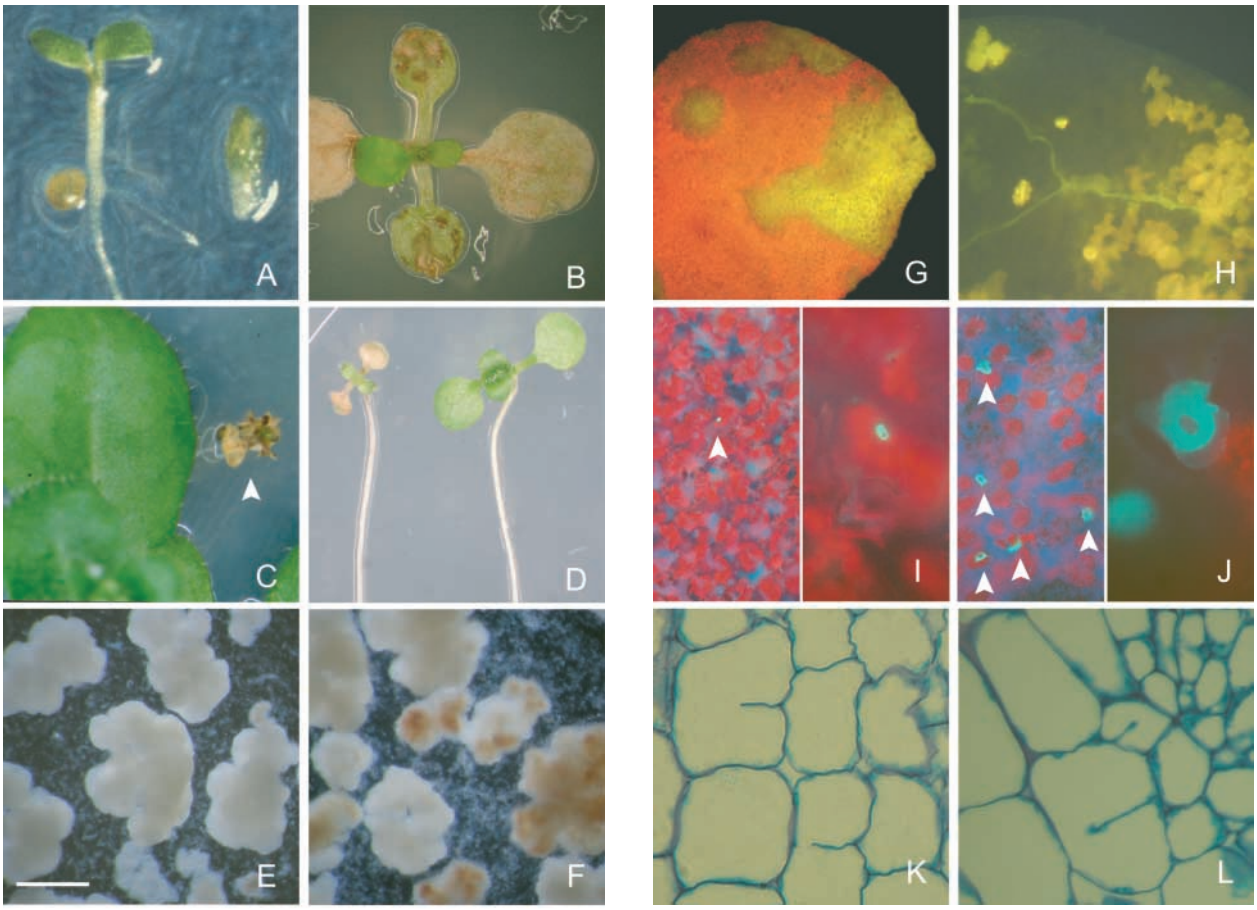

Figure 7. ***snp33* mutant phenotype.** (A–D) *snp33* seedling phenotypes. (A) *keu* mutant seedling (right) next to a 5-d-old wild-type or *snp33* mutant seedling (left). *snp33* mutants were indistinguishable from wild-type at this age. (B) 15-d-old *snp33* seedling with brownish lesions on cotyledons and rosette leaves. Note that the youngest leaves still look normal. (C) Size difference between *snp33* seedling (arrowhead) and wild-type sibling (left) after several weeks on plates. (D) Etiolated *snp33* (left) and wild-type (right) seedlings. After germination and etiolation in the dark, the seedlings were grown in the light to distinguish mutant and wild-type on the basis of brownish lesions. (E and F) Callus culture generated from wild-type (E) and *snp33* seedlings (F). Note brownish speckles in F. (G and H) Yellow autofluorescence of *snp33* mutant tissue observed in blue light. (G) Tip of a young rosette leaf; the red fluorescence is caused by chlorophyll. (H) Detail of a cotyledon after ethanol-acetic acid fixation, which eliminates chlorophyll autofluorescence. Single fluorescing cells can be distinguished easily. (I and J) Aniline blue staining of wild-type (I) and *snp33* (J) cotyledons observed in ultraviolet light. Callose depositions fluoresce bright turquoise, chlorophyll red. Left, overviews, callose depositions marked by arrowheads; right, close-ups. Note that callose depositions are significantly larger in the *snp33* mutant than in wild-type. (K and L) Partially divided cells of a 9-d-old *snp33* mutant seedling seen on 3-μm sections stained with toluidine blue. Details from the petiole of a cotyledon (K) and the hypocotyl/petiole junction (L). Bar: (E and F) 1 mm; (G) 500 μm; (H) 125μm; (I and J, left) 150 μm; (I and J, right) 15 μm; (K and L) 12 μm.

Considering the extreme dwarf phenotype of *snp33* mutant plants, we examined whether growth was affected directly. Dark-grown wild-type seedlings are long and slender due to extreme cell elongation in the hypocotyl. In this assay, *snp33* mutants were indistinguishable from wild-type (Fig. 7 D), indicating that cell expansion is not severely affected. The same seems true for cell division, since a vividly proliferating callus culture could be established from mutant seedlings. *snp33* callus only differed from wild-type by the occasional deposition of brownish material reminiscent of the lesions in the aerial parts of mutant plants (Fig. 7, E and F). This is in contrast to the strong cytokinesis mutants *kn* and *keu* which do not proliferate in callus culture under equivalent conditions.

Although the overall appearance of *snp33* seedlings differed strongly from the seedling phenotype of *kn* or *keu* (Fig. 7 A), the microscopic analysis of toluidine blue–stained sections indicated cytokinesis defects also for *snp33* (Fig. 7, K and L). In *snp33* mutant seedlings, partially divided cells occurred at a higher frequency than in wild-type as determined from longitudinal sections of hypocotyls and cotyledonary petioles. Whereas wild-type on average showed only 0.15 incomplete cell walls per section (n = 150 sections), the corresponding frequency for the *snp33* mutant was 3.6 (n = 163 sections), that is, ~25 times higher. Thus, the mutant analysis suggests that SNP33 is functionally involved in cytokinesis but also in other processes as indicated by the necrotic phenotype.

keu snp33 double mutant analysis

Despite their strong cell division defects during embryogenesis, *kn* and *keu* single mutants develop to the seedling stage (Assaad et al., 1996; Lukowitz et al., 1996; Fig. 7 A). How-

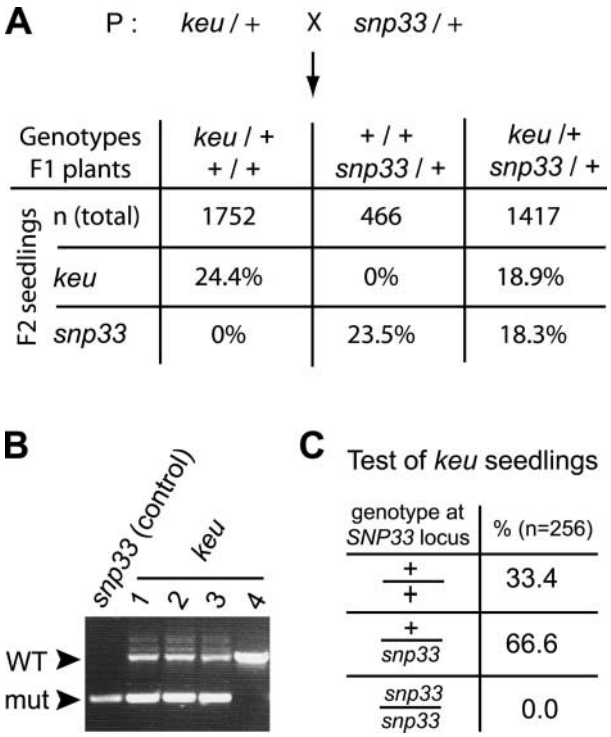

Figure 8. **Analysis of *snp33 keu* double mutants.** (A) A heterozygous *keu* plant was crossed to a heterozygous *snp33* plant, and the segregation rates of *keu* and *snp33* mutant seedlings in the F2 were compared. Note ~5% shortage of each of the mutant phenotypes among the progeny of doubly heterozygous F1 plants compared with those of the singly heterozygous F1 plants. italic, mutant alleles; +, wildtype allele. (B and C) *keu* seedlings from a doubly heterozygous F1 plant were genotyped at the *SNP33* locus. (B) Amplification products of the three-primer PCR used for genotyping (example). The lower band (mut) indicates the presence of the *snp33* mutant allele, and the upper band (WT) indicates the presence of the *SNP33* wild-type allele. snp33 (control), seedling displaying the *snp33* mutant phenotype; *keu*, four *keu* seedlings from a doubly heterozygous F1 plant (1–3, heterozygous at the *SNP33* locus; 4, homozygous wild-type). (C) Determination of the *SNP33* genotype of 256 *keu* seedlings from a doubly heterozygous F1 plant.

ever, cytokinesis is blocked completely in the *kn keu* double mutant, resulting in single-celled multinucleate embryos (Waizenegger et al., 2000). Therefore, we examined whether a combination with *keu* might also enhance the weak cytokinesis defects seen in *snp33* mutants. Among the seedling progeny of a selfed *keu*/+;*snp33*/+ plant, the frequencies of the two single mutant phenotypes, *keu* and *snp33*, were reduced by ~5% compared with single mutant sister lines (Fig. 8 A). In addition, no novel seedling phenotype was observed, suggesting that the *keu snp33* double mutants died before germination. Alternatively, disregarding the observed segregation ratio, double mutant seedlings might resemble *keu* seedlings if their growth was arrested before the onset of *snp33* necrosis. To distinguish between these possibilities, we tested the *SNP33* genotype of *keu* seedlings from a doubly heterozygous mother plant. None of the 256 *keu* seedlings analyzed by PCR were homozygous for *snp33,* whereas *keu* seedlings heterozygous for *snp33* occurred at the expected frequency (Fig. 8, B and C). Thus, *keu snp33* double mutants indeed did not reach the seedling stage. A comparable analysis for *snp33* in combination with *kn* was hampered by the variable germination rate of *kn* mutants and an unreliable PCR on the very small *kn* seedlings. However, we obtained preliminary data that indicate a similar effect as for the *keu snp33* double mutant (unpublished data).

SNP33 is a member of a small protein family in *Arabidopsis*

No SNP33 protein was detected in *snp33* mutant tissue (Fig. 2) even after overexposure of the Western blots, indicating that the mutant represents a complete loss of function. Thus, residual gene function does not account for the rather weak cytokinetic phenotype of *snp33* mutants. Sequencing of the *Arabidopsis* genome identified two additional SNAP25 homologous genes, *AtSNAP29* (AGI-ID: At5g07880) and *AtSNAP30* (AGI-ID: At1g13890). The deduced proteins show ~62% identity to AtSNAP33 and 52% identity among each other (Fig. 9), which raised the issue of functional redundancy. Therefore, we tested their ability to interact with the KN syntaxin in the yeast two-hybrid assay (Fig. 10). All three SNAP25 homologues of *Arabidopsis* interacted with the KN cytoplasmic region, suggesting that cytokinetic defects of *snp33* single mutants may be weakened by activities of the other SNAP25 homologues.

Discussion

Our search for interactors of the cytokinesis-specific syntaxin KN identified the t-SNARE AtSNAP33 (SNP33), a member of a small family of SNAP25 homologous proteins in *Arabidopsis*. We characterized *SNP33* by expression pattern and subcellular localization of the protein and by phenotypic and genetic analysis of a loss-of-function mutant. Our data suggest that SNP33 is involved in several processes, including cytokinesis, and that its function in cytokinesis may be replaced partially by other SNAP25 homologues.

Membrane association of AtSNAP33

In cell fractionation experiments, SNP33 was tightly associated with membranes from which it was only removed by detergent thus behaving like an integral membrane protein. How SNP33 associates with membranes is an open question. Unlike most SNAREs, SNAP25-type proteins lack a membrane-spanning domain, but some SNAP25 homologues attach to membranes via a lipid membrane anchor (Steegmaier et al., 1998). A conserved cysteine cluster has been shown to be palmitoylated and responsible for initial membrane association of SNAP25 (Veit et al., 1996). However, this cluster is not present in SNP33. It is also missing in mammalian SNAP29 and the yeast SNAP25 homologues Sec9p and Spo20p, but in contrast to SNP33, Sec9p and SNAP29 can be extracted from membranes with high pH (Brennwald et al., 1994; Steegmaier et al., 1998), suggesting that they do not carry a lipid anchor at all. Whether SNP33 is lipid modified at its only cysteine at position 119 or at another residue remains to be investigated.

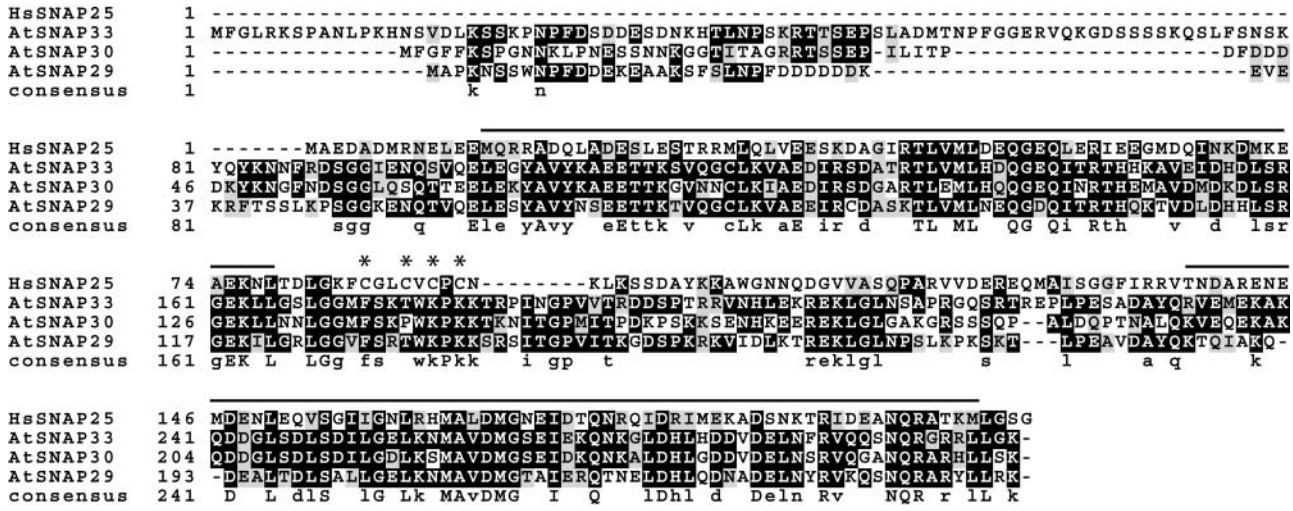

Figure 9. **Protein sequence alignment of *Arabidopsis* SNAP25 homologues.** Human SNAP25 was aligned with the three SNAP25 homologues of *Arabidopsis*. The lines above the sequences indicate the α-helical regions possibly involved in SNARE complex formation. The conserved cysteine residues of HsSNAP25 involved in palmitoylation are marked by asterisks. Consensus: capital letters, residues conserved in all four proteins; small letters, residues conserved among the three *Arabidopsis* homologues. The sequence data are available from GenBank/EMBL/DDBJ under accession nos: HsSNAP25, NP_003072; AtSNAP29, CAB62600; AtSNAP30, AAF79396; AtSNAP33, BAB10383.

Subcellular localization studies indicated that SNP33 is localized predominantly at the plasma membrane and cell plate of dividing cells. Additional weaker labeling in the cytoplasm may represent cytosolic or endomembrane-bound protein. In support of the latter, BFA treatment, which leads to an agglomeration of endomembranes, resulted in an accumulation of SNP33 label in distinct patches within the cell that were marked also by the transmembrane protein PIN1. The SNP33-labeled endomembranes may be transit compartments to the plasma membrane or endosomes.

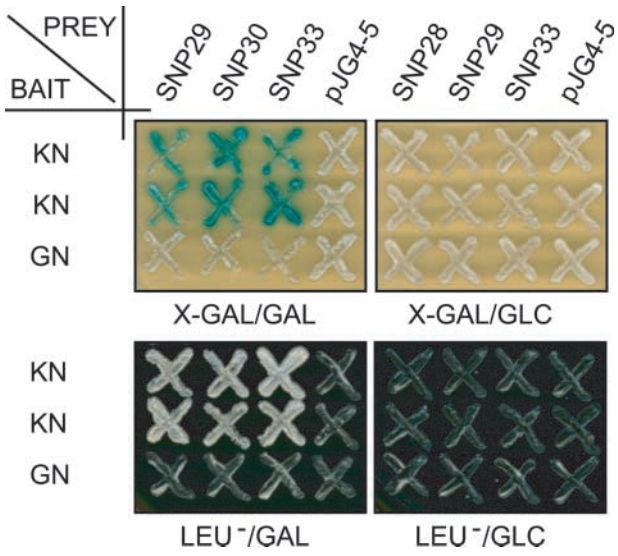

Figure 10. **Interaction of KN with different *Arabidopsis* SNAP25 homologues.** Using the two-hybrid system, the cytoplasmic domain of KN was tested for interaction with full-length constructs of the *Arabidopsis* SNAP25 homologues. GNOM (GN) bait and empty prey vector (pJG4-5) were used as negative controls. Two independent clones are shown when KN was used as the bait. Interaction was tested in the color assay on X-gal containing plates (top, X-Gal) and in the growth assay on medium lacking leucine (Leu⁻, bottom). Interaction was only observed upon induction of the prey constructs with galactose (left, GAL) and not on glucose-containing plates (right, GLC).

A role for SNP33 in cytokinesis

We demonstrated that SNP33 interacts with the cytokinesis-specific syntaxin KN under different experimental conditions, implying a role for SNP33 in cell division. In addition, both proteins colocalized at the forming cell plate, which strongly suggests that the interaction observed in vitro reflects the situation in vivo. Functional data also support a role for SNP33 in cytokinesis. The phenotypic analysis of *snp33* mutant plants revealed incomplete cell walls as expected for cytokinesis defects, and double mutants of *snp33* and the strong cytokinesis mutant *keu* displayed synthetic embryo lethality, suggesting that both proteins promote the same process. Interestingly, synthetic embryo lethality has also been observed for *kn keu* double mutants (Waizenegger et al., 2000), whereas both single mutants develop until the seedling stage. Both, SNP33 and KEU are members of small gene families in *Arabidopsis*, which suggests a simple mechanistic interpretation of the double mutant data. In this scenario, KEU function can in part be fulfilled by a KEU homologue if SNP33 is present, and SNP33 can be substituted by a SNP33 homologue if KEU is present. However, the two substitutes are fully incompatible with one another such that a functional pathway is blocked completely in the *keu snp33* double mutant. This does not imply necessarily that SNP33 and KEU interact directly, although Sec1p has been shown to bind to the core fusion complex in yeast (Carr et al., 1999).

Implications for a SNARE complex in cell plate formation

In plant cytokinesis, vesicle fusion plays a prominent role in the formation and lateral expansion of the cell plate. Although the

identification of the cytokinesis-specific syntaxin KN demonstrated the involvement of a SNARE complex in cell plate formation, its exact composition has not been resolved. Since KN lacks orthologues in nonplant organisms, it was conceivable that the cytokinetic SNARE complex might have a unique composition. Our characterization of SNP33 suggests that the cytokinetic SNARE complex consists of a syntaxin and a SNAP25 homologue thus resembling trimeric SNARE complexes acting at the plasma membrane in yeast and mammals, in contrast to tetrameric complexes found preferentially on endomembranes (Fukuda et al., 2000). This similarity suggests that cell plate formation is a variant of exocytosis. An analogous situation has been reported for yeast where related SNARE complexes mediate exocytosis at the plasma membrane of vegetative cells and membrane fusion during sporulation, a process described as similar to plant cytokinesis (Neiman, 1998). In yeast, both SNARE complexes use the same syntaxins and synaptobrevins but employ functionally distinct SNAP25 homologues, Sec9p in vegetative cells as opposed to Spo20p in sporulation (Neiman et al., 2000). By contrast, in *Arabidopsis* the syntaxin KN is a specific component of the cytokinetic SNARE complex, whereas the SNAP25 homologue SNP33 appears to be shared with other SNARE complexes (see below).

In summary, we propose that the specific KN syntaxin contributes one helix and the more general SNP33 adds two helices to the cytokinetic fusion complex. Assuming that the number of helices in SNARE core complexes is invariant, it will be important to determine what protein, general or specific, contributes the fourth helix to this bundle.

Other roles for SNP33

In plants, no SNARE complexes at the plasma membrane have been described, although candidates for plasma membrane syntaxins have been proposed (Sanderfoot et al., 2000). Because of its subcellular localization and its ubiquitous cell cycle–independent expression, SNP33 is a likely component of a general SNARE complex at the plant plasma membrane in addition to its role in cytokinesis. This assumption is supported by the finding that SNP33 binds at least one syntaxin other than KN in the yeast two-hybrid assay (unpublished data). The mammalian SNAP25 homologues, especially SNAP29, also seem to be binding partners for a variety of syntaxins (Steegmaier et al., 1998). Furthermore, some features of the *snp33* lack-of-function mutant, such as the formation of necrotic lesions, autofluorescence, and enhanced localized callose deposition, cannot be related easily to defects in cytokinesis but are rather reminiscent of a heterogeneous class of mutants collectively called disease lesion mimics (Dietrich et al., 1994). Some of these mutants are related to pathogen response, whereas others are perturbed in cellular metabolism, with lesions occurring at specific developmental stages (Hu et al., 1998), as also observed for *snp33*. Thus, SNP33 function may become especially important at a particular developmental stage, most likely due to a lack of redundancy (see below). Although mutations in a growing number of genes result in disease lesion mimicry, *snp33* is the first to affect vesicle fusion. How the latter defect causes the lesion phenotype remains to be investigated.

Specificity and redundancy of SNAP25 homologues

The ubiquitous expression of SNP33 contrasts with its more restricted requirement as revealed by the mutant phenotype, indicating that its function is nonessential in some contexts. One possible explanation would be that other proteins perform overlapping functions. We envision a scenario in which there is perfect redundancy of SNP33 function in a field A, such as embryo viability, partial redundancy in a field B, such as cytokinesis, and insufficient redundancy in a field C, which finally causes death of the *snp33* mutant. AtSNAP29 and AtSNAP30 might substitute for SNP33 in cell division, since they interacted also with KN in the yeast two-hybrid assay, and the corresponding mRNAs were represented in cDNA libraries made from proliferating tissues.

Sequence analysis of the *Arabidopsis* genome revealed extensive segmental duplication, possibly reflecting an ancient tetraploidization event (The *Arabidopsis* Genome Initiative, 2000). For example, AtSNAP29 and AtSNAP33 are located in a duplicated region of ~100 kb (K. Mayer, personal communication), indicating that once in plant evolution they had the same function. Derivative copies of an ancestral gene may have retained the original regulation and function or may have specialized. A striking example of overlapping function involving three genes is found in flower development of *Arabidopsis*. In the triple mutant *sepallata 1/2/3*, organ identity is changed to sepals in all whorls of the flower, whereas each single mutant displays only a very subtle phenotype (Pelaz et al., 2000). Redundancy might also be valid for the SNAP25 family at least in certain processes, such as cytokinesis. By contrast, *Arabidopsis* syntaxins seem to be more unique. In addition to *kn*, which shows severe cytokinetic aberrations already early in embryonic development (Lukowitz et al., 1996), four other *Arabidopsis* syntaxin mutants have been described (*syp21-2*, *syp22*, *syp41*, and *syp42*) (Sanderfoot et al., 2001). Homozygous mutant progeny could be identified for none of the latter, implying that each has essential functions.

Conclusion

Our data suggest that SNP33, the first SNAP25 homologue functionally characterized in plants, cooperates with the KN syntaxin and the KEU Sec1 homologue during cell plate formation. Further analysis will reveal to what extent SNP33 is involved in SNARE complex formation at the plasma membrane and how SNP33 function relates to the observed disease lesion mimic phenotype. In addition, the SNAP25 family of *Arabidopsis* will be an excellent model to study the extent and significance of functional redundancy among members of small gene families that are involved in basic cellular processes.

Materials and methods

Yeast two-hybrid assay

We used the lexA-based interaction-trap system as described in Ausubel et al. (1995). An *Arabidopsis* cDNA library generated from young siliques (Grebe et al., 2000) was screened for KN-interacting proteins using the yeast strain EGY-48 and the lacZ reporter pSH18-34. KN cytoplasmic domain (amino acids 1–287) was amplified from cDNA and cloned into the bait vector pEG202 using restriction sites added by PCR (EcoRI/BamHI). In the screen, 1.8×10^6 primary transformants were replated by 2×10^7 colonies on leu^- medium; 1041 clones were grown after 4 d, and 96 of these also showed galactose-dependent activation of the lacZ reporter and were further analyzed. Restriction digests of the prey inserts amplified by PCR

allowed grouping into 24 classes, and sequencing showed that three classes represented clones of different length derived from the gene *AtSNAP33 (SNP33).* To test for interaction of full-length SNP33, AtSNAP30, and AtSNAP29 with KN, the prey vector pJG4-5 was modified. The internal BamHI site was destroyed, and a new BamHI site was inserted in frame into the EcoRI site of the polylinker. The SNAP25 homologues were amplified from cDNA and cloned via BamHI/XhoI into the modified pJG4-5. Restriction sites were added by PCR. The bait construct lexA-$GNOM_{18–45}$ (Grebe et al., 2000) was used as a negative control.

Plant material and growth conditions

The *snp33* mutation was induced in *Arabidopsis thaliana* ecotype Wassilewskija. The *keu* allele AP77, ecotype Landsberg *erecta,* was used in the double mutant analysis.

Plants were grown as described previously (Mayer et al., 1991). To generate callus cultures, 30–50 seedlings were transferred into 100 ml liquid medium (4.3 g/liter MS salts, 0.5 g/liter MES, 3% sucrose, 1× Gamborg's B5 vitamins [Duchefa], 1 mg/liter 2,4-D and 0.25 mg/liter kinetin, pH 5.8) and incubated at 20°C in constant light with agitation. When sufficient callus material had developed, the cultures were split into two, once a week, and supplemented with new medium. The suspension culture used in GST pulldown experiments was a kind gift of the John Innes Centre (Norwich, UK) and was propagated as described previously (Fuerst et al., 1996).

For the in vitro root culture, 10-d-old plantlets were transferred to liquid medium (0.46% MS salts, 0.018% KH_2PO_4, 0.02% myo-inositol, 0.001% thiamin, 0.0001% pyridoxin, 0.0001% biotin, 0.0002% glycin, 0.0001% nicotinic acid, 0.00005% folic acid, 3% sucrose, pH 5.8) and incubated for 3 wk in darkness with slow agitation. Then, the roots were cut, transferred to the same liquid medium, and grown in the dark. Every 4 wk, the roots were divided in four parts and transferred to fresh medium.

Preparation of microsomes and solubilization of SNP33

5 g of roots cultivated in vitro were homogenized on ice with mortar and pestle in 4 ml of 50 mM 3-morpholinopropanesulfonic acid buffer, pH 7.6, containing 0.5 M sorbitol, 10 mM EGTA, 2.5 mM potassium metabisulfite, 4 mM salicylhydroxylamic acid, 5% polyvinylpyrrolidone, and 1% BSA. The mixture was filtered through miracloth and centrifuged at 8,000 *g* for 15 min at 4°C. The supernatant was centrifuged at 100,000 *g* for 30 min at 4°C. To test for solubilization of SNP33, the 100,000 *g* pellet was resuspended in 10 mM phosphate buffer, pH 7.6, containing 0.5 M sorbitol. The suspension was divided in five aliquots, which contained either 2 M urea, 1% sodium dodecyl sulfate, 1 M NaCl, 0.1 M Na_2CO_3, pH 11.0, or 10 mM phosphate buffer, pH 7.6, and incubated for 30 min at room temperature. Half of each aliquot was kept, which represents the total membrane, and the other half was centrifuged at 100,000 *g* for 1 h at 4°C. Supernatant and total membrane were analyzed by SDS-PAGE and Western blots.

In vitro binding of SNP33 and KN

Full-length *SNP33* was cloned into pGEX-4-T1 (Amersham Pharmacia Biotech) via BamHI/XhoI restriction sites added by PCR. The cytoplasmic domain of KN (amino acid 1–284) was cloned into pGEX-4-T1 via addition of EcoRI/XhoI restriction sites. GST pulldown experiments were performed as described previously (Grebe et al., 2000).

Immunofluorescence and Western blot analysis

Whole-mount immunofluorescences, preparation of protein extracts, and Western blots were performed as described in Lauber et al. (1997). The anti-KN serum (Lauber et al., 1997) was used at 1:6,000 for Western blots and at 1:4,000 for immunofluorescence analysis. The anti-PIN1 serum (Gälweiler et al., 1998) was used at 1:200. Myc-AtSNAP33 was detected with the mouse monoclonal anti–c-myc antibody 9E10 (Santa Cruz Biotechnology, Inc.) at 1:250. The anti-SNP33 serum was used at 1:4,000 and was generated as follows: a 6×His tag was added to the NH_2 terminus of SNP33, leading to the sequence MRGSHHHHHH followed by amino acids 8–300 of SNP33. Recombinant His-SNP33 was expressed in *Escherichia coli* XL-1 and purified via nickel affinity chromatography under denaturing conditions following the manufacturer's instructions (QIAGEN). The eluted protein was purified further via SDS-PAGE. A band of the correct size was cut from a gel stained in 0.3 M $CuCl_2$ for 10–20 min. After destaining by several changes of 0.25 M Tris, pH 8.0, 0.25 M EDTA, the protein was eluted from the squashed gel matrix in PBS, pH 7.3, and concentrated using a centrifugal concentrator (Macrosep, 10K9; Pall Filtron). Rabbit immunization was performed as described in Lauber et al. (1997). Unpurified serum of the third bleeding was used in all experiments. Secondary antibodies were used at the following dilutions: HRP-conjugated anti–rabbit IgG at 1:2,000 for Western blots (Boehringer) and anti–rabbit-FITC at 1:250, anti–rabbit-Cy3™ at 1:600, and anti–mouse-Cy3™ at 1:600 for immunofluorescence analysis (Dianova). Whole-mount immunofluorescences were analyzed using a confocal laser scanning microscope (Leica) and the Leica TCS-NT software.

T-DNA insertion lines screen

For T-DNA structure and experimental procedures used in the insertion line screen, see Bechtold et al. (1993). The T-DNA insertion line of *SNP33* (originally called EFS396) was detected in the DNA pool 307A using the *SNP33* genomic primer GMS25BW5 (5′-AGTCCAAACCTCCACTCTCTGATAAGC-3′) and the T-DNA primer TAG3 (5′-CTGATACCAGACGTTGCCCGCATAA-3′).

Plant transformation constructs and plant transformation

For cloning the *SNP33* genomic rescue constructs, we modified the plant transformation vector pGPTV-HPT (Becker et al., 1992) by deleting the GUS gene via an EcoRI/XbaI digest and religating the blunted vector (pGPTV-HPTmod). The resulting polylinker was EcoRI-XbaI-SalI-HindIII. The genomic fragments of *SNP33* were derived from the P1 clone MAF19 (*A. thaliana*, ecotype Columbia). Rescue construct A (Fig. 4) is a 5-kb EcoRI fragment cloned into pGPTV-HPTmod. For rescue construct B (Fig. 4), a 4.8-kb EcoO109I (blunted)/XhoI fragment was ligated into an EcoRI (blunted)/SalI cut pGPTV-HPTmod-vector. The myc tag was inserted into an unique SalI site of fragment B using the overlapping oligos MYC-sense (5′-TCGATGGAGCT*GAGCAAAAGCTTATTTCTGAGGAGGATCTTCTT*GCTGGATCAG-3′) and MYC-antisense (5′-TCGACTGATCCAGC*AAGAAGATCCTCCTCAGAAATAAGCTTTTGCTC*AGCTCCA-3′). Nucleotides coding for the c-myc epitope are written in italics. For the pSNP33–GFP construct, a 2.1-kb promotor fragment of SNP33 (Fig. 4, fragment C, ecotype Landsberg *erecta*) was amplified using the primers 5′-GGAGATATCGGAGGAAGAATGCAAGC-3′ and 5′-GGAGGATCCACAAAAGGAACACTTGG-3′, fused with the cDNA of mGFP5-ER (Haseloff et al., 1997), and ligated into the binary vector pBin19. Expression of the *pAtSNAP33–GFP* transgene was analyzed with the Leica DM R microscope, and pictures were taken with the CCD camera AxionCam (ZEISS) and analyzed with the software Axion Vision 2.05. The floral-dip method (Clough and Bent, 1998) was used for *Agrobacterium*-mediated plant transformation.

Determination of the *SNP33* genotype

The genotype of plants from rescue experiments was determined by PCR using the *SNP33* genomic primers GMS25FW1 (5′-TCCATCTTCTTCTTCACGGACTCCAC-3′) and GMS25BW2 (5′-GAGTGGTTCTCGGGTTCTTGATTGTC-3′). This PCR yielded only a product if no T-DNA was present in the *SNP33* gene. To differentiate between the endogenous Wassilewskija wild-type allele and the Columbia rescue construct, a SpeI restriction polymorphism was used. Only the Columbia fragment was cut. Plants from the rescue experiment using the myc-SNP33 construct were analyzed using the primer pair GMS25FW4 (5′-GCTAGATCCTGGGCTTTCGATTTG-3′) and 48SP2 (5′-GAACCGACTGGTTTTCAATACCACC-3′), which only gave a product if no T-DNA was inserted in *SNP33*. The myc-tagged fragment could be distinguished from the endogenous wild-type *SNP33* allele by a 54 bp length difference. To genotype *keu* seedlings for SNP33 in the double mutant analysis, a three-primer PCR was used, involving the SNP33 genomic primers GMS25FW4 and 48SP2 and the T-DNA primer TAG3. A 340-bp fragment resulted from the presence of the T-DNA insertion, and a 730-bp band indicated a *SNP33* allele without the insertion (Fig. 8).

Phenotypic analysis

Plantlets were analyzed using a Leica MZ125 binocular and a ZEISS microscope. Pictures were taken with a digital camera (Coolpix 990; Nikon). Autofluorescence was analyzed by observation in blue light (450–490 nm). Callose deposition was monitored by staining with aniline blue (45 min, 0.5 mg/ml in water) and observation in ultraviolet light. For sectioning, seedlings were fixed overnight in 4% paraformaldehyde in PBS, dehydrated via an ethanol series, and embedded in LR-White resin (London Resin Company, Ltd.). 3-μm sections were cut using a Leica microtome (Supercut 2065) and stained for 20 s with 0.1% toluidine blue, 0.1% borate. Stained sections were embedded in Eukitt (Kindler GmbH).

Other techniques

Molecular techniques were performed according to Ausubel et al. (1995) or the manufacturer's protocol. All constructs cloned via a PCR-based step were

confirmed by sequencing using the ABI PRISM BigDye Terminator cycle sequencing kit and the ABI sequencer 310 (Applied Biosystems). Sequence analysis was carried out with Vector NTI™ (Informax). Alignments were done with the ClustalW algorithm (Thompson et al., 1994). Images were processed with Adobe Photoshop® 6.0 and Adobe Illustrator® 9.0 software.

We thank Laurence Charrier for excellent technical assistance, H. Schwarz (Max-Planck-Institut für Entwicklungsbiologie, Tübingen, Germany) for rabbit immunization, K. Palme (Max Delbrück Laboratory, Cologne, Germany) for a kind gift of the anti-PIN1 serum, Jim Haseloff for the cDNA of mGFP5-ER, and David Bouchez, Michael Lenhard, Niko Geldner, and Arp Schnittger for helpful comments and critical reading of the article.

This work was supported by the European Union Biotechnology Program and the Deutsche Forschungsgemeinschaft grant SFB 446/B8. X. Gansel and L. Sticher were supported by grant 31-39595.93 from the Swiss National Foundation for Scientific Research.

Submitted: 30 July 2001
Revised: 30 August 2001
Accepted: 4 September 2001

References

The *Arabidopsis* Genome Initiative. 2000. Analysis of the genome sequence of the flowering plant *Arabidopsis thaliana. Nature.* 408:796–815.

Assaad, F., U. Mayer, G. Wanner, and G. Jürgens. 1996. The *KEULE* gene is involved in cytokinesis in *Arabidopsis*. *Mol. Gen. Genet.* 253:267–277.

Assaad, F., Y. Huet, U. Mayer, and G. Jürgens. 2001. The cytokinesis gene *KEULE* encodes a Sec1 protein that binds the syntaxin KNOLLE. *J. Cell Biol.* 152: 531–544.

Ausubel, F.M., R. Brent, R.E. Kingston, D.D. Moore, J.G. Seidmann, J.A. Smith, and K. Struhl. 1995. Current Protocols in Molecular Biology. John Wiley, New York.

Bechtold, N., J. Ellis, and G. Pelletier. 1993. In planta *Agrobacterium* mediated gene transfer by infiltration of adult *Arabidopsis thaliana* plants. *CR Acad. Sci. Série III, Sciences de la Vie.* 316:1194–1199.

Becker, D., E. Kemper, J. Schell, and R. Masterson. 1992. New plant binary vectors with selectable markers located proximal to the left T-DNA border. *Plant Mol. Biol.* 20:1195–1197.

Blatt, M.R., B. Leyman, and D. Geelen. 1999. Tansley review no. 108: molecular events of vesicle trafficking and control by SNARE proteins in plants. *New Phytologist.* 144:389–418.

Brennwald, P., B. Kearns, K. Champion, S. Keranen, V. Bankaitis, and P. Novick. 1994. Sec9 is a SNAP-25-like component of a yeast SNARE complex that may be the effector of Sec4 function in exocytosis. *Cell.* 79:245–258.

Burgess, R.W., D.L. Deitcher, and T.L. Schwarz. 1997. The synaptic protein syntaxin1 is required for cellularization of *Drosophila* embryos. *J. Cell Biol.* 138:861–875.

Carr, C.M., E. Grote, M. Munson, F.M. Hughson, and P.J. Novick. 1999. Sec1p binds to SNARE complexes and concentrates at sites of secretion. *J. Cell Biol.* 146:333–344.

Clough, S.J., and A.F. Bent. 1998. Floral dip: a simplified method for *Agrobacterium*-mediated transformation of *Arabidopsis thaliana. Plant J.* 16:735–743.

Dietrich, R.A., T.P. Delaney, S.J. Uknes, E.R. Ward, J.A. Ryals, and J.L. Dangl. 1994. *Arabidopsis* mutants simulating disease resistance response. *Cell.* 77: 565–577.

Fuerst, R.A., R. Soni, J.A. Murray, and K. Lindsey. 1996. Modulation of cyclin transcript levels in cultured cells of *Arabidopsis thaliana. Plant Physiol.* 112: 1023–1033.

Fukuda, R., J.A. McNew, T. Weber, F. Parlati, T. Engel, W. Nickel, J.E. Rothman, and T.H. Sollner. 2000. Functional architecture of an intracellular membrane t-SNARE. *Nature.* 407:198–202.

Gälweiler, L., C. Guan, A. Müller, E. Wisman, K. Mendgen, A. Yephremov, and K. Palme. 1998. Regulation of polar auxin transport by AtPIN1 in *Arabidopsis* vascular tissue. *Science*. 282:2226–2230.

Geldner, N., J. Friml, Y.-D. Stierhof, G. Jürgens, and K. Palme. 2001. Auxin-transport inhibitors block PIN1 cycling and vesicle trafficking. *Nature.* In press.

Glotzer, M. 1997. Cytokinesis. *Curr. Biol.* 7:R274–R276.

Grebe, M., J. Gadea, T. Steinmann, M. Kientz, J.U. Rahfeld, K. Salchert, C. Koncz, and G. Jürgens. 2000. A conserved domain of the *Arabidopsis* GNOM protein mediates subunit interaction and cyclophilin 5 binding. *Plant Cell.* 12:343–356.

Haseloff, J., K.R. Siemering, D.C. Prasher, and S. Hodges. 1997. Removal of a cryptic intron and subcellular localisation of green fluorescent protein are required to mark transgenic *Arabidopsis* brightly. *Proc. Natl. Acad. Sci. USA.* 94:2122–2127.

Hu, G., N. Yalpani, S.P. Briggs, and G.S. Johal. 1998. A porphyrin pathway impairment is responsible for the phenotype of a dominant disease lesion mimic mutant of maize. *Plant Cell.* 10:1095–1105.

Jantsch-Plunger, V., and M. Glotzer. 1999. Depletion of syntaxins in the early *Caenorhabditis elegans* embryo reveals a role for membrane fusion events in cytokinesis. *Curr. Biol.* 9:738–745.

Lauber, M., I. Waizenegger, T. Steinmann, H. Schwarz, U. Mayer, I. Hwang, W. Lukowitz, and G. Jürgens. 1997. The *Arabidopsis* KNOLLE protein is a cytokinesis-specific syntaxin. *J. Cell Biol.* 139:1485–1493.

Lecuit, T., and E. Wieschaus. 2000. Polarized insertion of new membrane from a cytoplasmic reservoir during cleavage of the *Drosophila* embryo. *J. Cell Biol.* 150:849–860.

Lin, R.C., and R.H. Scheller. 2000. Mechanisms of synaptic vesicle exocytosis. *Annu. Rev. Cell Dev. Biol.* 16:19–49.

Lukowitz, W., U. Mayer, and G. Jürgens. 1996. Cytokinesis in the *Arabidopsis* embryo involves the syntaxin-related *KNOLLE* gene product. *Cell.* 84:61–71.

Mayer, A., R.A. Torrez-Ruiz, T. Berleth, S. Misera, and G. Jurgens. 1991. Mutations affecting body organization in the *Arabidopsis* embryo. *Nature.* 353: 402–407.

McNew, J.A., F. Parlati, R. Fukuda, R.J. Johnston, K. Paz, F. Paumet, T.H. Sollner, and J.E. Rothman. 2000. Compartmental specificity of cellular membrane fusion encoded in SNARE proteins. *Nature.* 407:153–159.

Misura, K.M., R.H. Scheller, and W.I. Weis. 2000. Three-dimensional structure of the neuronal-Sec1-syntaxin 1a complex. *Nature.* 404:355–362.

Nacry, P., U. Mayer, and G. Jürgens. 2000. Genetic dissection of cytokinesis. *Plant Mol. Biol.* 43:719–733.

Neiman, A.M. 1998. Prospore membrane formation defines a developmentally regulated branch of the secretory pathway in yeast. *J. Cell Biol.* 140:29–37.

Neiman, A.M., L. Katz, and P.J. Brennwald. 2000. Identification of domains required for developmentally regulated SNARE function in *Saccharomyces cerevisiae. Genetics*. 155:1643–1655.

O'Halloran, T.J. 2000. Membrane traffic and cytokinesis. *Traffic.* 1:921–926.

Otegui, M., and L.A. Staehelin. 2000. Cytokinesis in flowering plants: more than one way to divide a cell. *Curr. Opin. Plant Biol.* 3:493–502.

Pelaz, S., G.S. Ditta, E. Baumann, E. Wisman, and M.F. Yanofsky. 2000. B and C floral organ identity functions require *SEPALLATA* MADS-box genes. *Nature.* 405:200–203.

Pelham, H.R. 1999. SNAREs and the secretory pathway—lessons from yeast. *Exp. Cell Res.* 247:1–8.

Sanderfoot, A.A., F.F. Assaad, and N.V. Raikhel. 2000. The *Arabidopsis* genome. An abundance of soluble *N*-ethylmaleimide-sensitive factor adaptor protein receptors. *Plant Physiol.* 124:1558–1569.

Sanderfoot, A.A., M. Pilgrim, L. Adam, and N.V. Raikhel. 2001. Disruption of individual members of *Arabidopsis* syntaxin gene families indicates each has essential functions. *Plant Cell.* 13:659–666.

Satiat-Jeunemaitre, B., and C. Hawes. 1992. Redistribution of a Golgi glycoprotein in plant cells treated with brefeldin A. *J. Cell Sci.* 103:1153–1166.

Steegmaier, M., B. Yang, J.S. Yoo, B. Huang, M. Shen, S. Yu, Y. Luo, and R.H. Scheller. 1998. Three novel proteins of the syntaxin/SNAP-25 family. *J. Biol. Chem.* 273:34171–34179.

Steinmann, T., N. Geldner, M. Grebe, S. Mangold, C.L. Jackson, S. Paris, L. Galweiler, K. Palme, and G. Jürgens. 1999. Coordinated polar localization of auxin efflux carrier PIN1 by GNOM ARF GEF. *Science.* 286:316–318.

Straight, A.F., and C.M. Field. 2000. Microtubules, membranes and cytokinesis. *Curr. Biol.* 10:R760–R770.

Thompson, J.D., D.G. Higgins, and T.J. Gibson. 1994. CLUSTAL W: improving the sensitivity of progressive multiple sequence alignments through sequence weighting, position-specific gap penalties and weight matrix choice. *Nucleic Acids Res.* 22:4673–4680.

Veit, M., T.H. Sollner, and J.E. Rothman. 1996. Multiple palmitoylation of synaptotagmin and the t-SNARE SNAP-25. *FEBS Lett.* 385:119–123.

Waizenegger, I., W. Lukowitz, F. Assaad, H. Schwarz, G. Jürgens, and U. Mayer. 2000. The *Arabidopsis KNOLLE and KEULE genes* interact to promote vesicle fusion during cytokinesis. *Curr. Biol.* 10:1371–1374.

Waters, M.G., and F.M. Hughson. 2000. Membrane tethering and fusion in the secretory and endocytic pathways. *Traffic*. 1:588–597.

Weber, T., B.V. Zemelman, J.A. McNew, B. Westermann, M. Gmachl, F. Parlati, T.H. Sollner, and J.E. Rothman. 1998. SNAREpins: minimal machinery for membrane fusion. *Cell.* 92:759–772.